Applied Catalysis B: Environmental 189 (2016) 56–64

Contents lists available at ScienceDirect

Applied Catalysis B: Environmental

journal homepage: www.elsevier.com/locate/apcatb

Ru-Co(III)-Cu(II)/SAC catalyst for acetylene hydrochlorination

Haiyang Zhang[a], Wei Li[a], Yunhe Jin[a], Wei Sheng[a], Maocong Hu[c], Xianqin Wang[c,**], Jinli Zhang[a,b,*]

[a] Key Laboratory for Systems Bioengineering MOE, Tianjin University; Collaborative Innovation Center of Chemical Science and Chemical Engineering (Tianjin), Tianjin 300072, PR China
[b] School of Chemistry and Chemical Engineering, Shihezi University, Xinjiang, Shihezi 832003, PR China
[c] Department of Chemical, Biological and Pharmaceutical Engineering, New Jersey Institute of Technology, Newark, NJ 07102, USA

ARTICLE INFO

Article history:
Received 19 October 2015
Received in revised form 19 January 2016
Accepted 11 February 2016
Available online 15 February 2016

Keywords:
Acetylene hydrochlorination
Trimetallic Ru-based catalyst
Interaction
Catalytic activity

ABSTRACT

A series of trimetallic Ru-Co(III)-Cu(II)/SAC catalysts were synthesized and assessed for acetylene hydrochlorination, combining with characterizations of TPR, TPD, TGA, TEM, XPS, EXAFS, etc. Compared with the monometallic and bimetallic catalysts, the trimetallic Ru1Co(III)3Cu(II)1/SAC catalyst with 0.1 wt% Ru loading shows a superior activity with the acetylene conversion of 99.0%. It is illustrated that co-addition of Co(III) and Cu(II) can make the ruthenium active species dispersed highly on the carrier, and Cu(II) species can not only inhibit the reduction of $RuCl_3$ precursors, but also make Co^{2+} or Co° transform to high valent species of Co(III), resulting in more ruthenium oxides and low valent Cu^+/Cu° species. The Ru1Co(III)3Cu(II)1/SAC is a promising non-mercuric catalyst for acetylene hydrochlorination reaction with the advantages of environmental benign and low cost.

1. Introduction

Poly vinyl chloride (PVC), widely used in many engineering areas, is manufactured with vinyl chloride monomer (VCM) as the main raw material. Hydrochlorination of acetylene is an important process for the production of vinyl chloride in locations where coal-based economies remain active, though this method is largely superseded by ethylene based process in many other countries [1,2]. Mercury chloride supported on activated carbon (AC) has been employed as the industrial catalyst for this process for many years [3–5]. However, the catalyst deactivates rapidly due to the loss of volatile active components ($HgCl_2$, Hg) and the poisonous mercuric compounds would do harm to both environment and human health [6–9]. According to the latest Minamata Convention signed in Japan, the application of mercuric chloride is forbidden by the UN Environment Programme's Governing Council in 2020. Hence, it is necessary to develop a new non-mercury catalyst with high activity and selectivity for acetylene-based PVC manufacture process in coal-rich regions.

Since Hutchings [10] firstly observed the relations between the catalyst activity and the standard electrode potential of the cations, Au catalysts had become attractive because of their superior activities compared with the industrially preferred mercuric chloride catalysts. Furthermore, Hutchings and his coworkers studied the reaction mechanism and found that initial treatment with C_2H_2 led to a lower activity, whereas pretreatment with HCl enhanced the initial activity [11–15]. However, the stability of the Au catalysts need to be promoted [12,14]. Second metal addition is an alternative way. Conte et al. investigated the effect of the noble metal addition including Pd, Pt, Ir and Rh, and demonstrated that these metals showed no positive effect on the conversion of acetylene while the Au catalyst alone was the most active catalyst [13]. Meanwhile, some researchers attempted to explore the effect of non-noble metals to the Au-catalysts. Zhang et al. [16] reported that an acetylene conversion of 92% could be achieved over 1 wt% Au1Co(III)3/SAC catalysts under the conditions of 150 °C, C_2H_2 gas hourly space velocity (GHSV) = 360 h^{-1}, C_2H_2/HCl feed volume ratio (V_{C2H2}/V_{HCl}) = 1:1.15 and no visible decline in activity was observed within 48 h. Wang et al. [17] established a kinetic model for acetylene hydrochlorination over the bimetallic Au-Cu/C catalyst where both conversion and selectivity of more than 99.5% and more than 200 h life time could be obtained under the conditions of 137–177 °C, the V_{HCl}/V_{C2H2} ratio of 1.10–1.15, and the total GHSV of 42–84 h^{-1}. Huang et al. [18] found TiO_2 could significantly enhance the stability of Au/C catalyst, and reported that

* Corresponding author.
** Corresponding author.
E-mail addresses: xianqin.wang@njit.edu (X. Wang), zhangjinli@tju.edu.cn (J. Zhang).

http://dx.doi.org/10.1016/j.apcatb.2016.02.030
0926-3373/

the acetylene conversion over $10TiO_2$–$AuCl_3$/AC catalyst declined from 92% to 81% after 10 h reaction under the temperature of 180 °C, the V_{C2H2}/V_{HCl} = 1:1.15 and GHSV(C_2H_2) = 870 h^{-1}. Zhou et al. [19] reported the acetylene conversion of catalyst AuBi (0.3 wt% Au and 0.95 wt% Bi) reached the highest 85%. However, so far the reported Au-based catalysts are not available in industrial PVC manufacture due to the high price of Au and the relative short lifetime of the catalysts. It is essential to develop non-noble metal based non-mercuric catalysts for acetylene hydrochlorination.

Base metals such as ruthenium, manganese, bismuth, cerium and cobalt were investigated for acetylene hydrochlorination [19–21]. Among these metals, ruthenium-based catalysts showed excellent reaction activity and stability. In particular, over Ru1Co(III)3/SAC catalysts an acetylene conversion of 95% was achieved at the reaction time of 48 h under the conditions of 170 °C, GHSV(C_2H_2) = 360 h^{-1}, V_{C2H2}/V_{HCl} = 1:1.1 [22]. However, the stability of current Ru-based catalysts was poor due to the loss of Ru active species and coke deposition during the reaction [21,22]. Therefore, these works enlightened us to study an effective modulation of ruthenium active species in Ru-Co(III)/SAC catalyst by adding a third metal, in order to explore a cheap Ru-based catalyst with long stability for acetylene hydrochlorination.

In this paper, the effects of Co(III) and Cu(II) additives on the performance of Ru-based catalysts were investigated in detail to improve the activity but also the stability of a relative cheap catalyst for acetylene hydrochlorination. Through characterizations of low temperature N_2 adsorption/desorption, TGA, TEM, CO-TPD, TPR, XRD, XPS and EXAFS techniques, it is illustrated that the trimetallic Ru1Co(III)3Cu(II)1/SAC is a promising non-mercuric catalyst for acetylene hydrochlorination reaction with the advantage of environmental benign and low cost.

2. Experimental

2.1. Catalyst preparation

The ruthenium-based catalysts were prepared by an incipient impregnation technique using the precursors involving $RuCl_3$, $CuCl_2$ and/or $Co(NH_3)_6Cl_3$ [13,23,24]. To prepare the precursor $Co(NH_3)_6Cl_3$, the mixture of $CoCl_2{\cdot}6H_2O$ and NH_4Cl, with the $CoCl_2{\cdot}6H_2O/NH_4Cl$ mass ratio of 3/2, was first dissolved quantitatively in the tri-distilled water at 60 °C and then cooled down to 10 °C. A solution of 25% $NH_3{\cdot}H_2O$ was added quantitatively, followed by adding a solution of 6% H_2O_2 with equal volume under stirring. Next, the overall mixture was incubated at 60 °C for 20 min to make the reaction completed, followed by the processes of suction filtration and dessication (150 °C, 12 h), generating the product of $Co(NH_3)_6Cl_3$.

Spherical activated carbon (SAC) (ShangHai Carbosino Material Co., Ltd., 20–40 mesh) was washed by a 1 mol/L HCl solution at 70 °C for 5 h to remove impurities, followed by washing with tri-distilled water to neutral pH and dessicating at 150 °C for 24 h, then the obtained clean SAC was used as the support. Monometallic Ru catalyst was prepared by impregnating quantitatively the clean SAC support with an aqueous solution of $RuCl_3$ at 60 °C under stirring for 16 h, the obtained mixture was dessicated at 150 °C for 18 h to prepare the monometallic Ru/SAC catalyst. When $CuCl_2$ or $Co(NH_3)_6Cl_3$ was added quantitatively into the aqueous solution of $RuCl_3$, the bimetallic catalysts of Ru-Cu(II)/SAC or Ru-Co(III)/SAC can be prepared through the above similar procedure. To prepare the trimetallic catalyst Ru-Co(III)-Cu(II)/SAC, certain amount of $Co(NH_3)_6Cl_3$ was first added into the hydrochloric acid solution of $RuCl_3$, and then $CuCl_2$ was added quantitatively under stirring to obtain a mixture solution of three precursors, which was adopted to impregnate the SAC support. The Ru loading of the catalysts was fixed at 0.1 wt% unless mentioned. To make the discussion clear, the catalyst was named with the Ru/Co/Cu molar ratio, i.e., the catalysts Ru1Co(III)1Cu(II)1/SAC, Ru1Co(III)3Cu(II)0.5/SAC, Ru1Co(III)3Cu(II)1/SAC, Ru1Co(III)3Cu(II)1.5/SAC and Ru1Co(III)5Cu(II)1/SAC denoted respectively the Ru/Co/Cu molar ratio of 1:1:1, 1:3:0.5, 1:3:1, 1:3:1.5, or 1:5:1. Similarly, the bimetallic catalysts of Ru1Co(III)3/SAC, Ru1Cu(II)1/SAC and Co(III)3Cu(II)1/SAC denoted respectively the Ru/Co molar ratio of 1:3, the Ru/Cu molar ratio of 1:1 and the Co/Cu molar ratio of 3:1. The monometallic catalysts of Ru/SAC, Co(III)/SAC, Cu(II)/SAC were also prepared as a control. In addition, the related catalysts were also prepared with the Ru loading of 1.0 wt% for catalyst characterizations.

2.2. Catalyst characterization

The absolute content of Ru in all the catalysts was measured with inductively coupled plasma-atomic emission spectrometry (ICP-AES) (710ES, Varian Company in USA).

Quantachrome Autosorb Automated Gas Sorption System (Quantachrome Instruments, USA) was used to conduct low-temperature N_2 adsorption/desorption experiments. The catalysts were heated at 250 °C and outgassed for 4 h at this temperature and measured using liquid nitrogen adsorption at −196 °C. Surface areas were determined by the BET method, the pore size distribution was calculated by the HK method.

In order to measure the amount of coke deposition on the used catalysts, thermogravimetric analysis (TGA) of the samples was performed by a NETZSCH STA 449F3 Jupiter® thermogravimetric-differential scanning calorimetry (TG-DSC) simultaneous thermal analyzer, flushing with an air flow rate of 30 mL/min. The temperature was increased from 25 to 800 °C with a heating rate of 10 °C/min.

Transmission electron microscopy (TEM) were recorded using a JEM2100F TEM and an FEI Titan 80–300 TEM/STEM equipped with CEOS spherical aberration corrector. Before each test, the sample was ground and dispersed in ethanol, followed by laying the droplets of the suspension on a TEM grid (300-mesh copper, holey carbon film)

Temperature programmed reduction (TPR) and CO pulse chemisorption (CO-TPD) experiments were performed using an AutoChem BET TPR/TPD (Quantachrome Instruments AMI-90) instrument. The weight of sample in a typical experiment was about 0.1 g. TPR experiments were carried out in a micro-flow reactor fed with a 10% H_2/Ar mixture at a flow rate of 30 mL/min. The temperature was ranged from 35 °C to 900 °C at a heating rate of 10 °C/min. For CO-TPD experiments, the sample was first reduced at 300 °C for 2 h in the atmosphere of 10% H_2/Ar at a flow rate of 30 mL/min and then cooled to room temperature. 250 μL pulses of 10% CO/He were introduced, and the CO uptake profile was measured using a TCD detector. The dispersion of Ru was calculated assuming a CO:Ru stoichiometry of 1:1.

X-ray diffraction (XRD) measurements were performed using a D8-Focus X-ray diffractometer (Bruker AXS, GER) with monochromatised Cu Kα radiation (λ = 1.5406 Å) operating in the 2θ scan ranged from 10° to 90°.

X-ray photoelectron spectroscopy (XPS) spectra were recorded by a Kratos AMICUS spectrometer (SHIMADZU, JP) selecting a monochromatised Al Kα X-ray source (24.2 W). All XPS spectra were recorded with a pass energy of 187.85 eV, and high resolution spectra with a pass energy of 46.95 eV. The spectral regions corresponding to Ru3p3, Co2p3 and Cu2p3 core levels were recorded for related sample. C1s line (284.6 eV) from the support was adopted as the calibration of the spectra.

Extended X-ray absorption fine structure (EXAFS) spectra of the Ru K-edge absorption were recorded at the EXAFS station of XDAC V1.4 Datafile V1. When measured, the electron energy was

Table 1
Catalytic performance of different monometallic catalysts.

Catalysts	Metallic loading content	X_A (%)	S_{VCM} (%)
Ru/SAC	1.0% (w)	78.0	99.6
Cu(II)/SAC	1.0% (w)	24.8	99.2
Co(III)/SAC	1.0% (w)	2.2	99.5
SAC	–	14.1	99.8

Note: Reaction conditions: T = 170 °C, V_{HCl}/V_{C2H2} = 1.10, GHSV(C_2H_2) = 180 h^{-1}, t = 48 h.

found to be 2.80 GeV. A cut-off Si(111) single crystal was used as a monochromator. Two ionisation chambers, filled with Ar, served as detectors. The electrochemical cell was positioned so that the electrode was exposed under a small angle to obtain maximum absorption in the thin-layer catalyst.

2.3. Catalytic testing

Catalyst tests were carried out in a fixed-bed flow microreactor (i.d. 10 mm). CKW-1100 temperature controller produced in the Chao Yang Automation Instrument Factory (Beijing, China) was used and the temperature was regulated. Before the reaction, nitrogen was used to remove water and air. Clean hydrogen chloride (99.9%) was dried using 5A molecular sieves, and acetylene (99.9%) was input into the silica-gel desiccant to remove trace impurities. C_2H_2 (15 mL/min) and HCl (16.5 mL/min) were then fed through the filter with a GHSV(C_2H_2) of 180 h^{-1} (5 mL catalyst) and the temperature was 170 °C. Under certain conditions, acetylene flow rate and the size of catalyst were changed to investigate the effect of mass transfer on the catalytic activity, and the results indicated that the effect of the external diffusion was eliminated at the C_2H_2 flow rate range of 25–100 mL/min; the reaction rate was not limited by the internal mass transport within the 0.180–0.900 mm (18–80 mesh) grain size range. The amount of catalyst in laboratory scale experiments is very low, and no significant development of hot spots occurs; moreover, the thermal conductivity of the catalyst is far higher than that of the outside air. Thus, the reaction had not been affected by the internal and external diffusion and heat transfer. The pressures of both HCl and C_2H_2 were in the safe and mild range of 1.1–1.2 bar [13,16]. The effluent of the reactor passed through the NaOH solution absorption bottle and then analyzed using a Beifen 3420A gas chromatograph.

3. Results and discussion

3.1. Effects of metal additives on the performance of Ru/SAC catalysts

Table 1 lists the catalytic performance of monometallic catalysts involving Ru/SAC, Co(III)/SAC, Cu(II)/SAC for acetylene hydrochlorination, besides the support SAC. Ru/SAC has the highest acetylene conversion of 78% among these monometallic catalysts. Then, on the basis of Ru/SAC, the additive of Co(III) and/or Cu(II) were adopted to improve the catalytic activity.

Fig. 1 displays the catalytic performance of the trimetallic catalysts Ru-Cu(II)-Co(III)/SAC with the same Cu/Ru ratio of 1:1 but different ratio of Co/Ru ranged from 0 to 5:1, under the conditions of 170 °C, the GHSV (C_2H_2) of 180 h^{-1}, V_{HCl}/V_{C2H2} = 1.10 and the Ru loading of 0.1 wt%. As the Co/Ru ratio is 0, the bimetallic catalyst Ru1Cu(II)1/SAC shows an acetylene conversion of 76.8% at 48 h (Fig. 1a), which is a little lower than that over Ru/SAC (Table 1). When the Co:Cu:Ru molar ratio equals 1:1:1, over the trimetallic catalyst Ru1Co(III)1Cu(II) 1/SAC, the acetylene conversion at 48 h is increased to 89.6%. As the Co:Cu:Ru molar ratio rises to 5:1:1 with 3:1:1 as the intermedia, the acetylene conversion

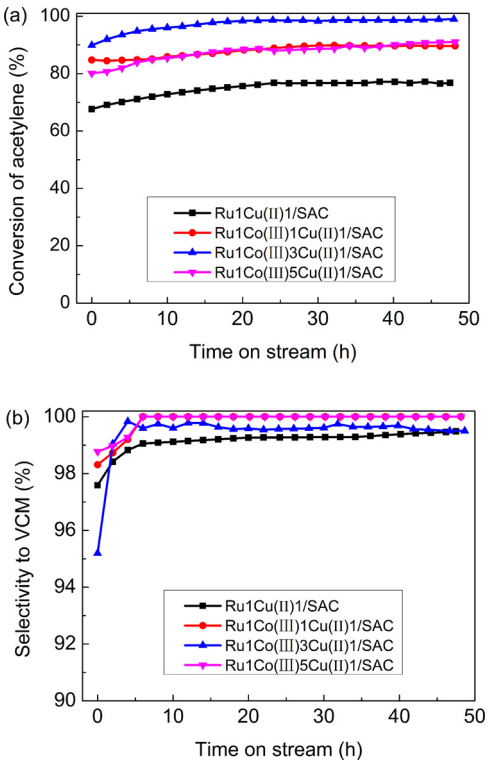

Fig. 1. The effect of Co(III) additive on the catalytic performance of trimetallic Ru-Cu(II)-Co(III)/SAC catalysts. Reaction conditions: T = 170 °C, GHSV(C_2H_2) = 180 h^{-1}, V_{HCl}/V_{C2H2} = 1.10, 0.1 wt% Ru loading.

achieves the highest value of 99.0% at 48 h over trimetallic catalyst Ru1Co(III) 3Cu(II)1/SAC, followed by the value of 91.0% over Ru1Co(III)5Cu(II)1/SAC. All these related catalysts show the selectivity to VCM above 99.0% at 48 h (Fig. 1b). It is indicated that the activity of Ru-based catalyst is improved obviously at the optimal Co/Ru ratio of 3:1.

We further studied the effect of Cu additives on the catalytic performance of trimetallic catalysts Ru-Cu(II)-Co(III)/SAC maintaining the same Co/Ru ratio of 3:1, under the same reaction conditions. As shown in Fig. 2, the acetylene conversion over Ru1Co(III)3/SAC is 86.7% at 48 h at the Cu/Ru ratio of 0 (Fig. 2a). When the Cu/Ru ratio increases from 0.5:1 to 1.5:1, the acetylene conversion increases and achieves the highest value of 99.0% at 48 h with the Cu/Ru ratio of 1:1; meanwhile the selectivity to VCM over all these catalysts are higher than 99%. The additives of Co(III) and Cu(II) species affect not only the valence state of ruthenium species but also the dispersion and coking deposition, which will be discussed in the following section. The excessive amounts of additives may occupy or cover the active sites on the catalyst instead, resulting in the decrease of catalytic activity. Therefore, there is a nonlinear dependence of the catalyst activity on Co and Cu content. Combining with Figs. 1 and 2, it is clear that the trimetallic catalyst Ru1Co(III)3Cu(II)1/SAC shows the superior activity and stability for acetylene hydrochlorination.

In order to obtain credible characterization results of these catalysts, the corresponding Ru-based catalysts with high Ru loading of 1.0 wt% and Co(III) 3Cu(II)1/SAC, in which the contents of Co(III) and Cu(II) are the same as that in Ru1Co(III)3Cu(II)1/SAC (1 wt% Ru) catalyst, were also prepared in this work. The activity of Ru/SAC, Ru1Cu(II)1/SAC, Ru1Co(III)3/SAC and Ru1Co(III)3Cu(II)1/SAC with Ru loading of 1 wt% were also assessed for acetylene hydrochlorination, as shown in Fig. S1. It is clear that the co-addition of Co and Cu species can also improve greatly the activity of 1 wt% Ru/SAC, approximate to their effects on the catalysts with low Ru loading of 0.1 wt%.

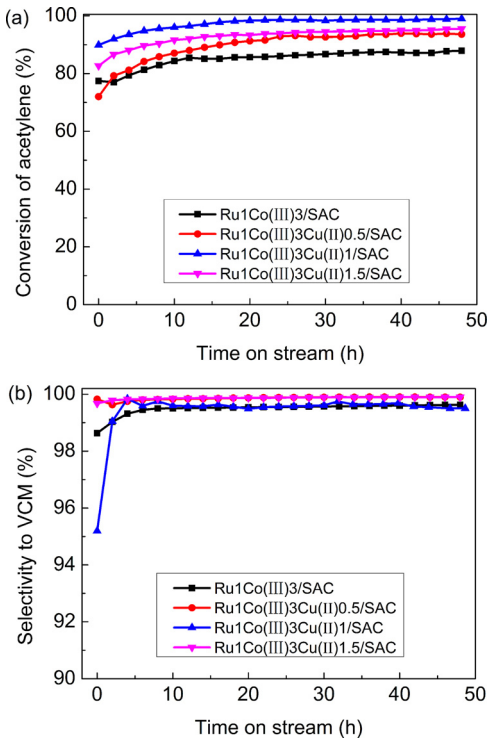

Fig. 2. The effect of Cu(II) additive on the catalytic performance of trimetallic Ru-Co(III)-Cu(II)/SAC catalysts. Reaction conditions: T = 170 °C, GHSV(C_2H_2) = 180 h^{-1}, V_{HCl}/V_{C2H2} = 1.10, 0.1 wt% Ru loading.

Table 2
Pore structure parameters of fresh catalysts with Ru loading of 1.0 wt%.

Catalyst	Surface area (m^2/g)		Total pore volume (cm^3/g)	
	Fresh	Used	Fresh	Used
SAC	1133	–	0.65	–
Ru/SAC	954	803	0.58	0.49
Ru1Cu(II)1/SAC	928	768	0.56	0.46
Ru1Co(III)3/SAC	873	780	0.52	0.46
Ru1Co(III)3Cu(II)1/SAC	829	759	0.49	0.45
Co(III)3Cu(II)1/SAC	882	771	0.53	0.46

3.2. Characterization of Ru-based catalysts

3.2.1. Catalyst texture properties

The low temperature N_2 adsorption-desorption experiments were carried out to measure the specific surface area and pore volume of the support and the fresh catalysts. The support SAC shows the type-I isotherms due to adsorption in the micropores [25]. And the 1.0 wt% Ru-based catalysts, including Ru/SAC, Ru1Cu(II)1/SAC, Ru1Co(III)3/SAC, Co(III)3Cu(II)1/SAC and Ru1Co(III)3Cu(II)1/SAC, display similar adsorption isotherms (Fig. S2a) and pore size distribution (Fig. S2b).

Table 2 lists the catalyst texture parameters of the Ru-based catalysts. The bare SAC has a specific surface area of 1133 m^2/g and a total pore volume of 0.65 cm^3/g. Fresh catalysts including Ru/SAC, Ru1Cu(II)1/SAC, Ru1Co(III) 3/SAC, Co(III)3Cu(II)1/SAC and Ru1Co(III)3Cu(II)1/SAC show the surface area and pore volume lower than those of the support SAC. This phenomenon, mentioned as the dilution effect previously [16], is attributed to the addition of active metallic components. The used catalysts exhibit lower surface areas and pore volumes, comparing with the fresh catalysts (Table 2). For the used Ru/SAC after experiencing 48 h reaction, the surface area decreases from the initial value of 954 m^2/g to 803 m^2/g, reducing about 15.8%. Similarly, the surface area of the used catalyst Ru1Cu(II)1/SAC shows a reducing fraction of 17.2%, for the used catalyst Co(III)3Cu(II)1/SAC there is a reducing about 12.6%, for the used catalyst Ru1Co(III)3/SAC there is a reducing about 10.7% and for the used Ru1Co(III)3Cu(II)1/SAC there is a reducing fraction of 8.4%. According to the activity shown in Fig. S1, the initial acetylene conversion is 87.6% over 1.0 wt% Ru/SAC, 79.4% over 1 wt% Ru1Cu(II)1/SAC, 26.9% over Co(III)3Cu(II)1/SAC, 90.7% over 1 wt% Ru1Co(III)3/SAC and 94.9% over 1 wt% Ru1Co(III)3Cu(II)1/SAC, which are decreased respectively to 76.4%, 64.5%, 16.3%, 90.6% and 94.5% after 48 h reaction. Therefore, it is reasonable to consider that for the used catalysts the loss of the surface area is probably attributed to the deposition of carbonaceous material on the catalyst surface [4], the loss of metal and the support and/or metal sintering, resulting in the decrease of the catalytic activity.

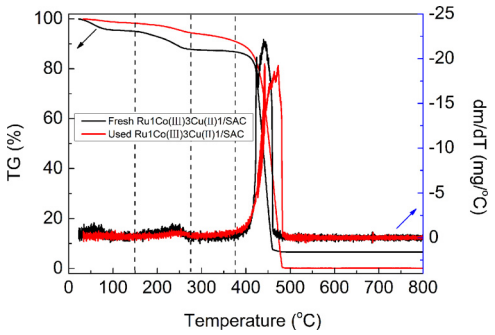

Fig. 3. TG and DTG curves of the fresh and used Ru1Co(III)3Cu(II)1/SAC catalysts with 1.0 wt% Ru loading.

Table 3
Coke deposition on the used 1.0 wt% Ru-based catalysts.

Catalyst	Amount of coke deposition (%)
Ru/SAC	6.3
Ru1Cu(II)1/SAC	7.4
Ru1Co(III)3/SAC	2.6
Ru1Co(III)3Cu(II)1/SAC	2.4
Co(III)3Cu(II)1/SAC	4.8

3.2.2. Coke deposition on the used catalysts

Fig. 3 shows the results of thermal gravimetric (TG) analysis of the fresh and used 1.0 wt% Ru1Co(III)3Cu(II)1/SAC catalysts. Both the fresh and used catalysts have a slight weight loss before 150 °C owing to the desorption of adsorbed water (Table S1). In the temperature range of 150–275 °C, there is an obvious weight loss (7.2%, Table S1) accompanied by an exothermic peak which is caused by the decomposition of certain compounds on the fresh catalysts under the atmosphere. As the temperature rises continuously from 275 to 375 °C, the fresh catalyst shows a weight loss of 1.0%, while the used catalyst has a loss of 3.4%. When the temperature exceeds 375 °C, there appears a rapid weight loss mainly due to the combustion of activated carbon. Thus, the coke burning may occur in the temperature range of 275–375 °C. Taking into account the SAC support can lose its weight by reacting with oxygen to emit CO_2, the amount of coke deposition is calculated by the difference of the weight loss between the fresh and the used catalysts in the temperature range of 275–375 °C [4,26]. Based on Fig. 3, the amount of coke deposition on the used Ru1Co(III)3Cu(II)1/SAC catalyst is calculated as 2.4%.

Similarly, the coke deposition on other used catalysts were also calculated via the corresponding TG and DTG curves (Fig. S3). As listed in Table 3, for the 1.0 wt% Ru-based catalysts, the amount of coke deposition increases in the order: Ru1Co(III)3Cu(II)1/SAC (2.4%) < Ru1Co(III)3/SAC (2.6%) < Co(III)3Cu(II) 1/SAC

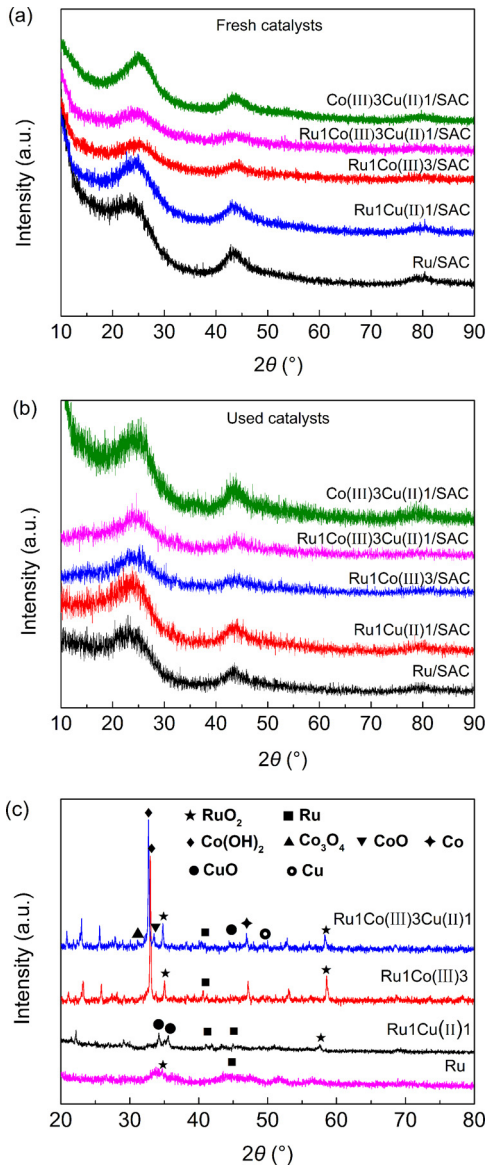

Fig. 4. XRD patterns of (a) fresh and (b) used Ru-based catalysts (1.0 wt% Ru loading), and (c) the unsupported precursors involving Ru, Ru1Cu(II)1, Ru1Co(III)3, Ru1Co(III)3Cu(II)1.

(4.8%) < Ru/SAC (6.3%) < Ru1Cu(II)1/SAC (7.4%), which is consistent with the variation tendency of surface area of used catalysts (Table 2). It is clear that the second metallic additive influences greatly the coke deposition, i.e., the Cu(II) additive alone makes the coke deposition increased, and the Co(III) additive dramatically reduces the coke deposition. However, compared with the monometallic Ru/SAC catalyst, the co-additive Co(III)-Cu(II) can greatly inhibit coke deposition, suggesting a synergy effect of the trimetallic Ru1Co(III)3Cu(II) 1/SAC.

3.2.3. *Effect of the additives on the dispersion of active species*

Fig. 4a and b display the XRD patterns of the fresh and used 1.0 wt% Ru-based catalysts. Besides the amorphous diffraction peaks of carbon, no discernible reflection is detected in the fresh Ru-based catalysts, indicating the high dispersion of active species. In order to understand deeply the potential active species of these catalysts, we characterized the individual precursor adopted to prepare each kind of Ru-based catalyst. Fig. 4c shows the XRD pattern of the unsupported precursor corresponding respectively to Ru, Ru1Cu(II)1, Ru1Co(III) 3, Ru1Co(III)3Cu(II)1. For the precursor to prepare Ru/SAC, i.e., Ru in Fig. 4c, there are peaks at 34° and 56.5° due to RuO_2, and the peak at 44.8° related to different crystal planes of Ru [27–29]. For the precursor to prepare Ru1Cu(II) 1/SAC (Ru1Cu(II)1 in Fig. 4c), there appears peaks of CuO besides RuO_2 and Ru species. For the precursor to prepare Ru1Co(III)3/SAC (Ru1Co(III)3 in Fig. 4c), there are peaks of $Co(OH)_2$, CoO and Co located respectively at 32.9°, 33.8° and 47.2°, as well as a small peak of Co_3O_4 besides the peaks of RuO_2 and Ru [30]. In the case of the precursor to prepare trimetallic Ru1Co(III)3Cu(II)1/SAC (Ru1Co(III)3Cu(II)1 in Fig. 4c), the XRD pattern is similar to that of Ru1Co(III)3 except of the additional peaks of CuO and Cu located respectively at 44.5° and 50°. It is illustrated that with the additives of Co and Cu can form certain active species with Ru, which influences significantly the activity of the related catalysts.

Fig. 5 and Fig. S4 display TEM images and the particle size distribution of the fresh and used Ru-based catalysts. It can be seen from Fig. 5a and Fig. S4a that the fresh Ru/SAC has numerous particles with the size about 2.6 nm on the carrier, which is consistent with the previous work [22]. Fig. 5c, e and g indicate that the fresh bimetallic catalysts Ru1Cu(II)1/SAC (Fig. S4c) and Ru1Co(III)3/SAC (Fig. S4e), and the trimetallic Ru1Co(III)3Cu(II)1/SAC (Fig. S4g) have small amount of particles with the size similar with those of Ru/SAC. After being experienced 48 h reaction, the used catalyst Ru/SAC possesses more particles with somewhat aggregation (Figs. 5b and S4b), while the used bimetallic and trimetallic catalysts do not show the aggregation of particles (Fig. 5d, f, and h). It is suggested that Co and Cu additives can make the Ru species dispersed well and retard the aggregation of active species, in accord with XRD patterns (Fig. 4).

In addition, the dispersion of Ru elements was estimated by the CO chemisorption experiments. As listed in Table 4, the Ru dispersion is 20.1% for the Ru/SAC catalyst. The Ru dispersion increases after the addition of other metal components, with the highest dispersion of 44.1% achieved in Ru1Co(III)3Cu(II) 1/SAC catalyst, followed by Ru1Cu(II)1/SAC (31.0%) and Ru1Co(III)3/SAC (24.1%). In combination with the TEM images, these data suggest that probably more Ru^{n+} ($n > 0$) species existed in the bimetallic and trimetallic Ru catalysts, which can not be discerned clearly in TEM images.

Table 4
Estimated Ru element dispersion in the fresh catalysts (1.0 wt% Ru) determined by CO chemisorption.

Catalyst	CO uptake/(μmol CO/g)	Ru dispersion/(%)
Ru/SAC	18.1	20.1
Ru1Cu(II)1/SAC	28.0	31.0
Ru1Co(III)3/SAC	21.8	24.1
Ru1Co(III)3Cu(II)1/SAC	40.0	44.1

Table 5
The loss ratio of Ru in Ru-based catalysts, determined by ICP-AES.

Catalyst	Ru loading/(wt%)		Loss ratio of Ru/(%)
	Fresh	Used	
Ru/SAC	0.909	0.878	3.41
Ru1Cu(II)1/SAC	0.911	0.890	2.31
Ru1Co(III)3/SAC	0.915	0.898	1.86
Ru1Co(III)3Cu(II)1/SAC	0.916	0.903	1.42

3.2.4. *Effect of the additives on the loss of Ru during the reaction*

Table 5 lists the ICP-AES analysis results of the Ru-based catalysts. It can be seen from Table 5 that all the catalysts have the similar content of Ru to the theoretical loading (1.0 wt%). The used catalysts exhibit lower content of Ru comparing with the fresh catalysts (Table 5). For the used Ru/SAC after experiencing 48 h reaction, the content of Ru decreases from the initial value

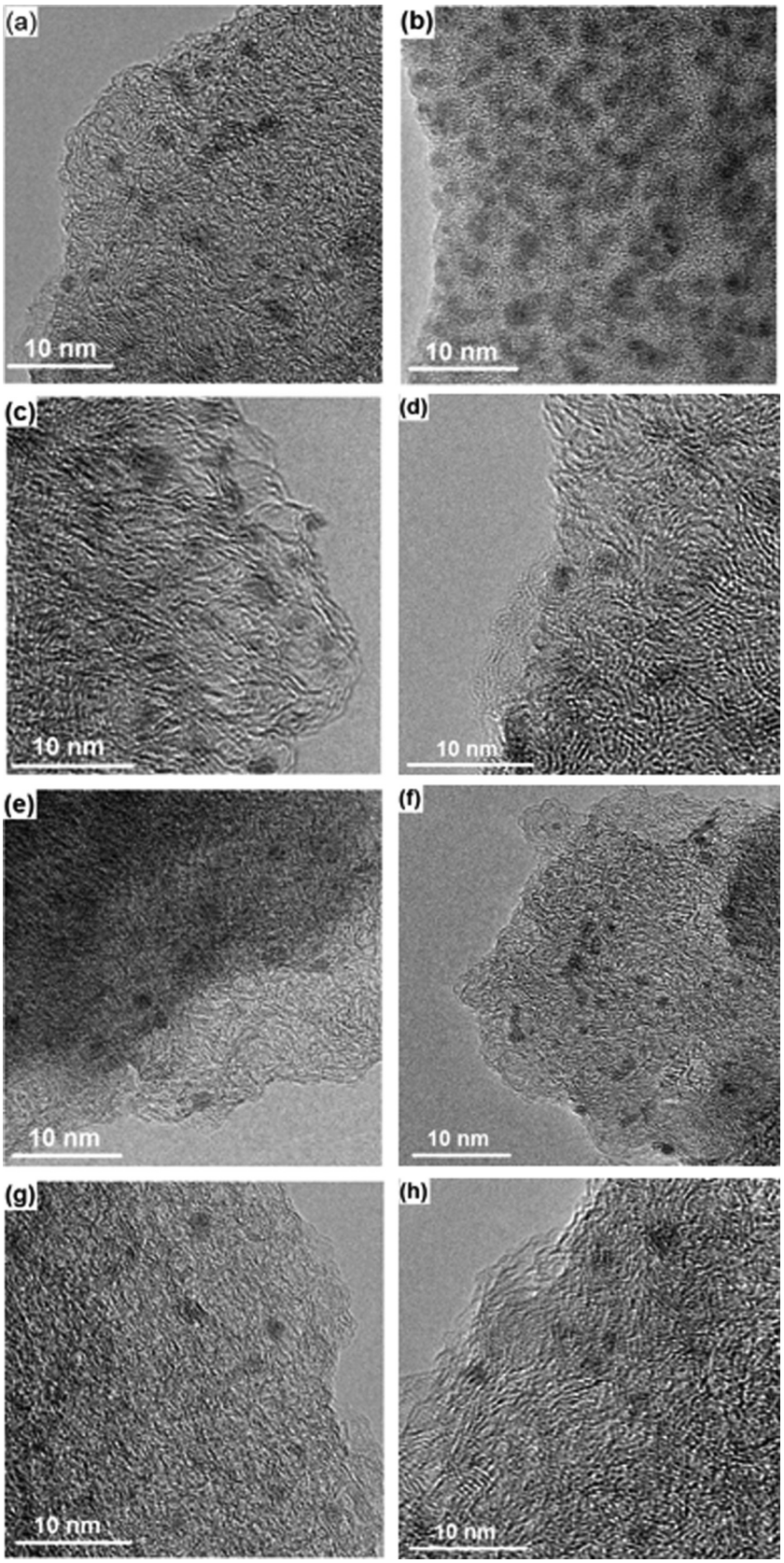

Fig. 5. TEM images of the fresh (a, c, e, and g) and used (b, d, f, and h) Ru-based catalysts with 1.0 wt% Ru loading. (a, b) Ru/SAC; (c, d) Ru1Cu(II)1/SAC; (e, f) Ru1Co(III)3/SAC; (g, h) Ru1Co(III)3Cu(II)1/SAC.

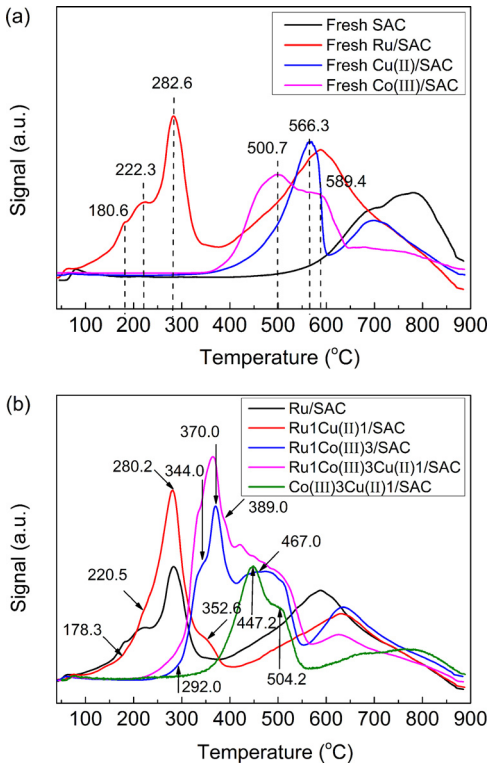

Fig. 6. H_2-TPR profiles of the fresh Ru-based catalysts with 1.0 wt% Ru loading.

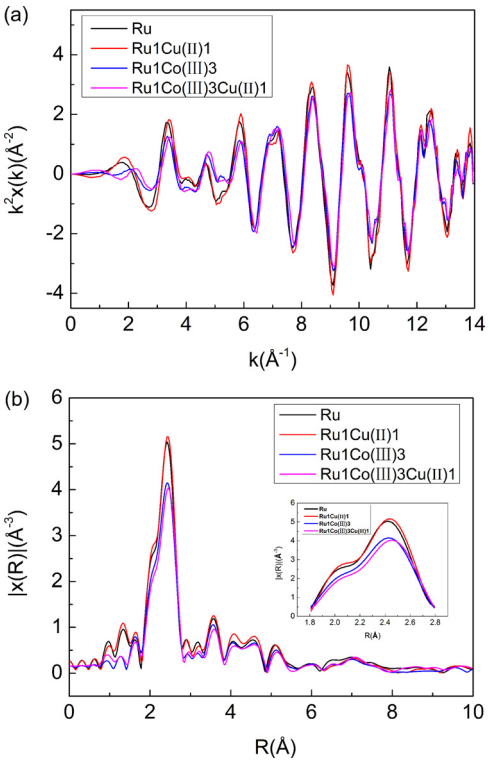

Fig. 7. Ru-K edge EXAFS signals (a) and the corresponding phase corrected Fourier transform (b) for unsupported Ru-based samples.

of 0.909–0.878%, reducing about 3.41%. Similarly, the Ru content of the used catalyst Ru1Cu(II)1/SAC shows a reducing fraction of 2.31%, for the used catalyst Ru1Co(III)3/SAC there is a reducing about 1.86% and for the used Ru1Co(III) 3Cu(II)1/SAC there is a reducing fraction of 1.42%. According to the activity shown in Fig. S1, the catalytic activity increases in the order: Ru1Cu(II)1/SAC < Ru/SAC < Ru1Co(III)3/SAC < Ru1Co(III)3Cu(II)1/SAC. Therefore, it is illustrated that to some extent, the loss of Ru active species may also be a factor in the decrease of catalyst activity, and the addition of Co(III) and Cu(II) additives contributes to the stabilization of active components.

3.2.5. *Effect of the additives on the reducibility of the Ru-based catalysts*

Fig. 6 shows TPR profiles of Ru-based catalysts. The carrier SAC shows only one H_2 consumption zone at temperature higher than 500 °C which would be mainly related to the decomposition of functional groups on the carrier (Fig. 6a). For the fresh catalysts, Ru/SAC exhibits a broad range between 100 °C and 350 °C with the peak center at 180.6 °C, 222.3 °C and 282.6 °C (Fig. 6a), corresponding to the reduction characteristics of RuO_x ($x > 2$), RuO_2 or Ru/RuO_y, and $RuCl_3$, respectively [27,28,31–35]. With the addition of Cu(II), a slight decrease of temperature in the reduction bands of Ru (178.3 °C, 220.5 °C, and 280.2 °C) and Cu (352.6 °C) species are observed. However, the existence of Co(III) significantly increases the reduction temperatures of RuO_x (292.0 °C), RuO_2 (344 °C), and $RuCl_3$ (370 °C). Trimetallic Ru1Co(III)3Cu(II)1/SAC catalyst has the TPR curve similar to that of Ru1Co(III)3/SAC, with the peak temperature shifted to lower values owing to the addition of Cu(II), except a reduction band of Cu species (389.0 °C). These shifts of reduction temperature indicate strong interactions between Ru and the additives of Co and Cu, in accord with the XRD pattern (Fig. 4c). It is worth mentioning that the amount of ruthenium oxides (RuO_y species in Ru/RuO_y was included) decreases in the following order: Ru1Co(III)3Cu(II)1/SAC > Ru1Co(III)3/SAC > Ru1Cu(II)1/SAC > Ru/SAC, indicating that the addition of Co(III) and Cu(II) species results in more amount of ruthenium oxides. It is illustrated that the Cu(II) additive may strengthen the relationship between Ru and Co species, and such synergic effect is important to improve the activity and the stability of Ru1Co(III)3Cu(II)1/SAC catalyst.

XPS spectra were obtained to further investigate the effects of Cu and Co additives on the Ru active species for the acetylene hydrochlorination reaction. Ru3p3/2 spectra is adopted to analyze the ruthenium species because of the overlapping between C1s and Ru3d signals [36]. There are more than one Ru species appeared (Fig. S5), the curve fitting is employed to determine the ratio of each Ru species [21,22,34,37]. As listed in Table 6, the monometallic Ru/SAC consists of 39.4% $RuCl_3$, followed by 32.1% RuO_2, 14.5% RuO_x and 14.0% Ru°. Bimetallic catalyst Ru1Cu(II)1/SAC has the dominant ruthenium species of 41.9% $RuCl_3$ followed by 39.9% ruthenium oxides (RuO_2 and RuO_x); there also appears a new ruthenium species of Ru/RuO_y at 462.2 eV with the content of 18.2%. Ru1Co(III)3/SAC has the major species of ruthenium oxides (51.6%) followed by $RuCl_3$ (37.8%), and the trimetallic catalyst Ru1Co(III)3Cu(II)1/SAC has the highest amount of ruthenium oxides (58.9%). It is suggested that Cu(II) additive can partially inhibit the reduction of $RuCl_3$ precursors, whereas Co(III) additive can interact closely with $RuCl_3$ precursors so as to form more amount of high valent ruthenium oxides in the catalysts. Moreover, there appears clearly the binding energy shifts of the Ru species in the presence of Cu(II) and Co(III) additives, confirming the strong interactions between ruthenium and additive components. In the case of used catalysts, the spectra are too noisy to clearly distinguish the peaks because of low loading of metals in the catalysts, and thus the deconvolution profiles of Ru were not provided.

Further, the deconvolutions of $Co2p_{3/2}$ and $Cu2p_{3/2}$ XPS spectra for the fresh catalysts was also conducted (Fig. S6 and Table 7). In the Ru1Co(III)3/SAC, Ru1Co(III)3Cu(II)1/SAC and Co(III)3Cu(II)1/SAC catalysts, there appears three Co species at

Table 6
The relative content and binding energy of Ru species in fresh catalysts with 1.0 wt% Ru loading, determined by XPS.

Fresh catalysts	Relative content (%)					Binding energy (eV)				
	Ru°	Ru/RuO_y	$RuCl_3$	RuO_2	RuO_x	Ru°	Ru/RuO_y	$RuCl_3$	RuO_2	RuO_x
Ru/SAC	14.0	0	39.4	32.1	14.5	461.1	–	463.9	465.7	468.0
Ru1Cu(II) 1/SAC	0	18.2	41.9	29.9	10.0	–	462.2	463.9	465.7	467.8
Ru1Co(III) 3/SAC	10.6	0	37.8	35.1	16.5	461.1	–	463.6	465.1	468.2
Ru1Co(III) 3Cu(II) 1/SAC	7.6	0	33.5	33.8	25.1	461.0	–	463.6	465.1	467.5, 471.1

Table 7
The relative content and binding energy of Cu and Co species in fresh catalysts with 1.0 wt% Ru loading, determined by XPS.

Fresh catalysts	Relative content (%)					Binding energy (eV)				
	$Cu^+/Cu°$	Cu^{2+}	Co°	Co^{2+}	Co^{n+} (n > 2)	$Cu^+/Cu°$	Cu^{2+}	Co°	Co^{2+}	Co^{n+}
Ru/SAC	0	0	0	0	0	–	–	–	–	–
Ru1Cu(II) 1/SAC	39.4	60.6	0	0	0	932.5	934.8	–	–	–
Ru1Co(III) 3/SAC	0	0	45.6	22.1	32.3	–	–	782.5	790.6	786.8
Ru1Co(III) 3Cu(II) 1/SAC	55.7	44.3	31.9	25.1	43.0	932.7	934.9	782.5	790.9	786.9
Co(III) 3Cu(II) 1/SAC	41.5	58.5	40.0	24.2	35.8	932.8	934.8	782.5	790.6	786.9

about 782 eV, 786 eV, and 790 eV, corresponding to Co°, Co^{n+} (n > 2), and Co^{2+}, respectively [38–40]. It can be seen from Table 7 that the relative content of Co species in Ru1Co(III)3/SAC decreases in the order: Co° (45.6%) > Co^{n+} (32.3%) > Co^{2+} (22.1%); similarly, the relative content of Co species in Co(III)3Cu(II)1/SAC decreases in the order: Co° (40.0%) > Co^{n+} (35.8%) > Co^{2+} (24.2%); while that in Ru1Co(III)3Cu(II)1/SAC catalyst decreases in the order: Co^{n+} (43.0%) > Co° (31.9%) > Co^{2+} (25.1%). The results indicate that the addition of Cu(II) contributes to maintain more high valent cobalt species in Ru-based catalysts. For the Cu species, copper existed in the oxidation state of Cu^{2+} in the Ru1Cu(II)1/SAC, Ru1Co(III)3Cu(II)1/SAC and Co(III)3Cu(II)1/SAC catalysts, as evidenced by the Cu 2p3/2 peak centered at 935.0 eV and the 2p → 3d satellite at 940–948 eV characteristic of Cu^{2+} with electron configuration of d9 [41–43]. The peak at 930–937.5 eV is discerned into two peaks. The position of the first peak is at about 932.6 eV, while the second one is situated at about 934.9 eV BE. The higher energy peak can be assigned to Cu^{2+}, while the lower energy peak could be related to Cu^+ or Cu° species [44,45]. It can also be seen from Table 7 that Ru1Cu(II)1/SAC and Co(III)3Cu(II)1/SAC possess the most Cu species of Cu^{2+} (60.6% and 58.5%), while Ru1Co(III)3Cu(II) 1/SAC possesses more low valent species of $Cu^+/Cu°$ (55.7%).

In summary, it is reasonable to conclude that the single Cu(II) additive can partially inhibit the reduction of $RuCl_3$ precursors, whereas the single Co(III) additive can interact closely with $RuCl_3$ precursors so as to form more highly valent ruthenium oxides in the catalysts, resulting in the formation of lower valent species of Co^{2+} or Co°. When both the additives were added simultaneously, Cu(II) species can not only inhibit the reduction of $RuCl_3$ precursors, but also make Co^{2+} or Co° transform to highly valent species of Co(III), resulting in more ruthenium oxides and low valent $Cu^+/Cu°$ species. Considering the observed activities of the catalysts (Ru1Cu(II)1/SAC < Ru/SAC < Ru1Co(III) 3/SAC < Ru1Co(III)3Cu(II)1/SAC (Figs. 1 and 2)), we may reasonably conclude that more ruthenium oxides contribute to higher catalytic activity.

3.2.6. *Influence of atoms nature on the catalyst*

Fig. 7a shows Ru-K edge EXAFS signals of unsupported Ru-based catalysts. It is indicated that the amplitude of signal shock decreases roughly in the following order: Ru1Cu(II)1 > Ru > Ru1Co(III)3 > Ru1Co(III)3Cu(II)1, suggesting that Ru1Cu(II) 1 has the largest co-ordination number while Ru1Co(III)3Cu(II)1 has the smallest one. Previously, it was reported that the trend of signal amplitude can reflect the similar change tendency of particle sizes [46]. Fig. 7b displays k^2 Fourier Transforms of the unsupported catalysts. The sequence of amplitude decrease is consistent with that shown in Fig. 7a. On the other hand, comparing the bond distance, it is illustrated that the peak at 2.0 Å is illustrated to Ru—O bond, and the peaks at 3.6 Å and 4.6 Å are due to Ru—Ru bond [47,48]. It is reported that the normal bond distance of free Ru-Cl was 2.3 Å and Ru-based alloy bond distance was about 2.4 Å [49]. Therefore the highest peak located around 2.4 Å is corresponding to the bond Ru—Cl associated with neighboring interactive components including Co(III), Cu(II), etc. Less co-ordination number and spare space structure could be expected on the lower amplitude catalyst. Furthermore, the interaction among atoms became easier and stronger than those higher amplitude catalysts. Therefore, the co-addition of Co(III) and Cu(II) can accelerate the electrophilic reagent attack, which is the key step of acetylene hydrochlorination. Consequently, the trimetallic catalyst shows the excellent catalytic performance.

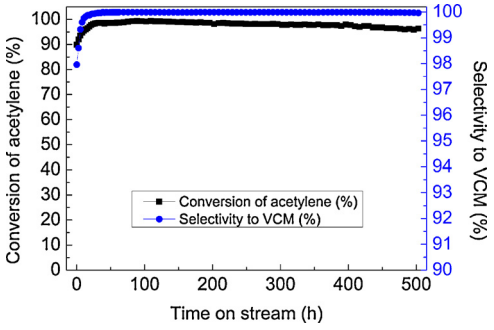

Fig. 8. The catalytic performance of Ru1Co(III)3Cu(II)1/SAC catalyst. Reaction conditions: T = 170 °C, GHSV(C_2H_2) = 90 h^{-1}, V_{HCl}/V_{C2H2} = 1.1, 0.1 wt% Ru loading.

3.3. *Long-term stability of trimetallic catalyst 0.1% Ru1Co(III)3Cu(II)1/SAC*

For the sake of economy and substantial industrial application, the long-term stability of trimetallic Ru1Co(III)3Cu(II)1/SAC catalyst with low Ru loading of 0.1 wt% was conducted. Fig. 8 shows the acetylene conversion and the selectivity to VCM at a lower GHSV(C_2H_2) of 90 h^{-1} as a function of reaction time. A short induction period at the beginning of the reaction is observed, and acetylene conversion reaches a maximum value of 99.3% within 80 h. Acetylene conversion then remained stable, and no obvious decline in 500 h was observed. In addition to the induction

period, the selectivity to VCM was close to 100% in the whole process. Moreover, compared with the noble metal catalysts, the trimetallic Ru-based catalyst enjoys a cost advantage; it also has a higher activity and a lower deactivation rate than the nonmetallic catalysts (Table S2). Thus, the results indicate that the economical Ru-Co(III)-Cu(II)/SAC catalyst could give favorable performance and the trimetallic catalyst may be promising in future application.

4. Conclusions

Trimetallic Ru-Co(III)-Cu(II)/SAC catalysts were synthesized and assessed for acetylene hydrochlorination reaction. The Ru1Co(III)3Cu(II)1/SAC catalyst shows the superior activity and good stability with the acetylene conversion of 99.0% and the selectivity to vinyl chloride of about 100% under the reaction conditions of 170 °C, V_{HCl}/V_{C2H2} = 1.10 and a C_2H_2 gas hourly space velocity of 180 h^{-1}. Through characterizations of low temperature N_2 adsorption/desorption, TGA, TEM, CO-TPD, TPR, XRD, XPS and EXAFS techniques, it is confirmed that co-addition of Co(III) and Cu(II) can make the ruthenium active components dispersed highly on the carrier and inhibit coke deposition; Co(III) and Cu(II) species can interact strongly with Ru species, and Co(III) additive can interact closely with $RuCl_3$ precursors so as to form more high valent ruthenium oxides in the catalysts, whereas Cu(II) species can not only inhibit the reduction of $RuCl_3$ precursors, but also make Co^{2+} or Co° transform to high valent species of Co(III), resulting in more ruthenium oxides and low valent Cu^+/Cu° species, although such kind of interaction may not be promoted when only Cu(II) was added. The Ru1Co(III)3Cu(II)1/SAC is a promising non-mercuric catalyst for acetylene hydrochlorination reaction with the advantage of environmental benign and low cost.

Acknowledgements

This work was supported by the Special Funds for Major State Research Program of China (2012CB720300), the Program for Changjiang Scholars and Innovative Research Team in University (No. IRT_15R46), NSFC (21176174) and the Start-Up Foundation for Young Scientists of Shihezi University (RCZX201507).

Appendix A. Supplementary data

Supplementary data associated with this article can be found, in the online version, at http://dx.doi.org/10.1016/j.apcatb.2016.02.030.

References

[1] X. Wei, H. Shi, W. Qian, G. Luo, Y. Jin, F. Wei, Ind. Eng. Chem. Res. 48 (2009) 128–133.
[2] L. Wang, F. Wang, J. Wang, X. Tang, Y. Zhao, D. Yang, F. Jia, T. Hao, Reac. Kinet. Mech. Cat. 110 (2013) 187–194.
[3] B. Nkosi, M.D. Adams, N.J. Coville, G.J. Hutchings, J. Catal. 128 (1991) 378–386.
[4] B. Nkosi, N.J. Coville, G.J. Hutchings, M.D. Adams, J. Friedl, F.E. Wanger, J. Catal. 128 (1991) 366–377.
[5] X. Li, M. Zhu, B. Dai, Appl. Catal. B: Environ. 142–143 (2013) 234–240.
[6] J. Zhang, Z. He, W. Li, Y. Han, RSC Adv. 2 (2012) 4814–4821.
[7] M. Conte, C.J. Davies, D.J. Morgan, T.E. Davies, D.J. Elias, A.F. Carley, P. Johnston, G.J. Hutchings, J. Catal. 297 (2013) 128–136.
[8] J. Ma, S. Wang, B. Shen, Reac. Kinet. Mech. Cat. 110 (2013) 177–186.
[9] H. Zhang, B. Dai, W. Li, X. Wang, J. Zhang, M. Zhu, J. Gu, J. Catal. 316 (2014) 141–148.
[10] G.J. Hutchings, J. Catal. 96 (1985) 292–295.
[11] G.J. Hutchings, D.T. Grady, Appl. Catal. 16 (1985) 411–415.
[12] M. Conte, A.F. Carley, C. Heirene, D.J. Willock, P. Johnston, A.A. Herzing, C.J. Kiely, G.J. Hutchings, J. Catal. 250 (2007) 231–239.
[13] M. Conte, A.F. Carley, G. Attard, A.A. Herzing, C.J. Kiely, G.J. Hutchings, J. Catal. 257 (2008) 190–198.
[14] M. Conte, A.F. Carley, G.J. Hutchings, Catal. Lett. 124 (2008) 165–167.
[15] M. Conte, C.J. Davies, D.J. Morgan, A.F. Carley, P. Johnston, G.J. Hutchings, Catal. Lett. 144 (2013) 1–8.
[16] H. Zhang, B. Dai, X. Wang, W. Li, Y. Han, J. Gu, J. Zhang, Green Chem. 15 (2013) 829–836.
[17] S. Wang, B. Shen, Q. Song, Catal. Lett. 134 (2010) 102–109.
[18] C. Huang, M. Zhu, L. Kang, X. Li, B. Dai, Chem. Eng. J. 242 (2014) 69–75.
[19] K. Zhou, W. Wang, Z. Zhao, G. Luo, J.T. Miller, M.S. Wong, F. Wei, ACS Catal. 4 (2014) 3112–3116.
[20] K. Zhou, J. Jia, X. Li, X. Pang, C. Li, J. Zhou, G. Luo, F. Wei, Fuel Process. Technol. 108 (2013) 12–18.
[21] Y. Pu, J. Zhang, L. Yu, Y. Jin, W. Li, Appl. Catal. A: Gen. 488 (2014) 28–36.
[22] J. Zhang, W. Sheng, C. Guo, W. Li, RSC Adv. 3 (2013) 21062–21068.
[23] B. Nkosi, N.J. Coville, G.J. Hutchings, Appl. Catal. 43 (1988) 33–39.
[24] B. Nkosi, N.J. Coville, G.J. Hutchings, J. Chem. Soc. Chem. Commun. 1 (1988) 71–72.
[25] J.M. Thomas, Catalyst Characterization, 1st ed., Chemical Industry Press, Beijing, 1981.
[26] Q. Song, S. Wang, B. Shen, J. Zhao, Pet. Sci. Technol. 28 (2010) 1825–1833.
[27] S. Huang, S. Chang, C.-t. Yeh, J. Phys. Chem. B 110 (2006) 234–239.
[28] Y. Liu, F. Huang, J. Li, W. Weng, C. Luo, M. Wang, W. Xia, C. Huang, H. Wan, J. Catal. 256 (2008) 192–203.
[29] V. Ragaini, C. Pirola, S. Vitali, G. Bonura, C. Cannilla, F. Frusteri, Catal. Lett. 142 (2012) 1452–1460.
[30] J. Wang, P.A. Chernavskii, A.Y. Khodakov, Y. Wang, J. Catal. 286 (2012) 51–61.
[31] P. Betancourt, A. Rives, R. Hubaut, C.E. Scott, J. Goldwasser, Appl. Catal. A: Gen. 170 (1998) 307–314.
[32] V. Mazzieri, F. Coloma-Pascual, A. Arcoya, P.C. L'Argentiere, N.S. Figoli, Appl. Surf. Sci. 210 (2003) 222–230.
[33] T. Stuchinskaya, M. Musawir, E. Kozhevnikova, I. Kozhevnikov, J. Catal. 231 (2005) 41–47.
[34] J.L. Gómez de la Fuente, M.V. Martínez-Huerta, S. Rojas, P. Hernández-Fernández, P. Terreros, J.L.G. Fierro, M.A. Peña, Appl. Catal. B: Environ. 88 (2009) 505–514.
[35] M. Ishikawa, M. Tamura, Y. Nakagawa, K. Tomishige, Appl. Catal. B: Environ. 182 (2016) 193–203.
[36] H. Xiong, Y. Zhang, K. Liew, J. Li, Fuel Process. Technol. 90 (2009) 237–246.
[37] R. Chetty, S. Kundu, W. Xia, M. Bron, W. Schuhmann, V. Chirila, W. Brandl, T. Reinecke, M. Muhler, Electrochim. Acta 54 (2009) 4208–4215.
[38] E. Iglesia, S.L. Soled, J.E. Baumgartner, S.C. Reyes, J. Catal. 153 (1995) 108–122.
[39] J.C. Dupin, D. Gonbeau, H. Benqlilou-Moudden, P. Vinatier, A. Levasseur, Thin Solid Films 384 (2001) 23–32.
[40] A.A. Khassin, T.M. Yurieva, V.V. Kaichev, V.I. Bukhtiyarov, A.A. Budneva, E.A. Paukshtis, V.N. Parmon, J. Mol. Catal. A: Chem. 175 (2001) 189–204.
[41] F. Raimondi, K. Geissler, J. Wambach, A. Wokaun, Appl. Surf. Sci. 189 (2002) 59–71.
[42] B.M. Nagaraja, A.H. Padmasri, B. David Raju, K.S. Rama Rao, J. Mol. Catal. A: Chem. 265 (2007) 90–97.
[43] B.M. Nagaraja, A.H. Padmasri, P. Seetharamulu, K. Hari Prasad Reddy, B. David Raju, K.S. Rama Rao, J. Mol. Catal. A: Chem. 278 (2007) 29–37.
[44] F. Severino, J.L. Brito, J. Laine, J.L.G. Fierro, A.L.o. Agudo, J. Catal. 177 (1998) 82–95.
[45] K.L. Deutsch, B.H. Shanks, J. Catal. 285 (2012) 235–241.
[46] K.I. Pandya, E.B. Anderson, D.E. Sayers, W.E. O'Grady, Le Journal de Physique IV 7 (1997), C2-955-C952-956.
[47] A. Rose, E.M. Crabb, Y. Qian, M.K. Ravikumar, P.P. Wells, R.J.K. Wiltshire, J. Yao, R. Bilsborrow, F. Mosselmans, A.E. Russell, Electrochim. Acta 52 (2007) 5556–5564.
[48] K.N. Loponov, V.V. Kriventsov, K.S. Nagabhushana, H. Boennemann, D.I. Kochubey, E.R. Savinova, Catal. Today 147 (2009) 260–269.
[49] I.V. Malakhov, S.G. Nikitenko, E.R. Savinova, D.I. Kochubey, N. Alonso-Vante, Nucl. Instrum. Methods Phys. Res. Sect. A 448 (2000) 323–326.